Cement & Concrete Composites 31 (2009) 613–621

Contents lists available at ScienceDirect

Cement & Concrete Composites

journal homepage: www.elsevier.com/locate/cemconcomp

Self-healing behavior of strain hardening cementitious composites incorporating local waste materials

S. Qian [a,*], J. Zhou [a], M.R. de Rooij [a,d], E. Schlangen [a], G. Ye [a,b,c], K. van Breugel [a]

[a] Faculty CITG, Delft University of Technology, Stevinweg 1, 2628 CN Delft, The Netherlands
[b] Southeast University, Sipailou 2, Nanjing, Jiangsu 210096, PR China
[c] Magnel Laboratory for Concrete Research, Department of Structural Engineering, Ghent University, Technologiepark-Zwijnaarde 904 B-9052, Ghent (Zwijnaarde), Belgium
[d] TNO Built Environment and Geosciences, van Mourik Broekmanweg 6, 2628 XE Delft, The Netherlands

ARTICLE INFO

Article history:
Received 6 November 2008
Received in revised form 17 March 2009
Accepted 19 March 2009
Available online 27 March 2009

Keywords:
Self-healing behavior
Strain hardening cementitious composites (SHCC)
Blast furnace slag
Limestone powder
Deflection capacity
Stiffness recovery

ABSTRACT

The self-healing behavior of a series of pre-cracked fiber reinforced strain hardening cementitious composites incorporating blast furnace slag (BFS) and limestone powder (LP) with relatively high water/binder ratio is investigated in this paper, focusing on the recovery of its deflection capacity. Four-point bending tests are used to precrack the beam at 28 days. For specimens submerged in water the deflection capacity can recover about 65–105% from virgin specimens, which is significantly higher compared with specimens cured in air. Similar conclusion applies to the stiffness recovery in water cured specimens. The observations under ESEM and XEDS confirmed that the microcracks in the specimens submerged in water were healed with significant amount of calcium carbonate, very likely due to the continuous hydration of cementitious materials. The self-healing cementitious composites developed in this research can potentially reduce or even eliminate the maintenance needs of civil infrastructure, especially when repeatable high deformation capacity is desirable, e.g. bridge deck link slabs and jointless pavements.

1. Introduction

Self-healing phenomenon has been observed in cementitious materials for many years. One such example is on an 18th century bridge in Amsterdam, where microcracks were self-healed by the recrystallization of calcite [1]. These observations suggest that under certain circumstances (e.g. when rainwater and carbon dioxide is available) concrete was able to heal its own damage (e.g. microcracks) with chemical products by itself. Furthermore, some researchers [2,3] noted a gradual reduction of permeability over time in the study of water flow through cracked concrete under a hydraulic gradient. These findings further reveal the ability of the cracked concrete to self-heal itself and slow the rate of water flow. The main cause of self-healing was attributed to the precipitation of calcium carbonate, a result of reaction between calcium ions from the concrete and carbon dioxide dissolved in water [2]. This type of self-healing mainly reduces the water permeability and is therefore most important to watertight structures, such as underground structures, reservoirs, and dams.

Besides permeability enhancement, many researchers also looked into the mechanical property recovery as a result of self-healing in concrete materials. For example, the recovery of flexural strength was observed in pre-cracked early age concrete beams while clamped and submerged in water [4]. Furthermore, it was observed that recovery of many mechanical related properties was possible after water immersion, e.g. the resonance frequency of an ultra high performance concrete damaged by freeze–thaw actions [5], the stiffness of pre-cracked specimens [6] and the compressive strength of pre-damaged cylindrical specimens [7]. The self-healing observed from these investigations was associated with continued hydration of the unhydrated cement or cementitious materials.

Other innovative methods, including encapsulation, expansive agents, and bacteria were also attempted by various researchers. The encapsulation approach was originated from the pioneering work by White and coworkers [8,9] who investigated the self-healing mechanism of polymeric materials. A number of experiments were conducted using this approach to release the encapsulated chemicals [10,11] into concrete cracks, therefore the damaged concrete can be repaired to certain extent. Recently wood/plant fiber was proposed by de Rooij et al. [12] as a carrier of self-healing agent to take advantage of the relatively large lumen as well as the wide availability of the wood fiber. Another approach, partial cement replacement with expansive agents was proposed and investigated by Kishi et al. [13] for crack self-closure by recrystallization of carbonates. Yet another approach, suggested by the experiments of Bang et al. [14] and

* Corresponding author.
E-mail address: zephyor@gmail.com (S. Qian).

0958-9465/$ - see front matter © 2009 Elsevier Ltd. All rights reserved.
doi:10.1016/j.cemconcomp.2009.03.003

Jonkers and Schlangen [15], used microorganisms to induce calcite precipitation in concrete. These novel concepts represent creative pathways to inducing highly desirable self-healing phenomena in concrete materials.

As suggested by many previous studies [2,3,16-19], the crack width of the concrete material was found to be critical for self-healing to take place. The requirement of crack width to promote self-healing falls roughly below 200 μm and preferably lower than 50 μm [20], especially for self-healing based on ongoing hydration of cement. Yet in practice, such small crack width is very difficult to achieve consistently in normal concrete structures, if not possible at all. The commonly used method of steel reinforcement has been called into question in recent years on its reliability. As a result, the ACI 318 code [21] has all together eliminated the specification on allowable crack width.

To achieve controlled tight crack width, a new class of fiber reinforced strain hardening cementitious composites, termed as engineered cementitious composites (ECC) has been developed by Li and continuously evolved over the last 15 years [22]. ECC has been deliberately engineered using micromechanics theory to possess self-controlled crack width that does not depend on steel reinforcement or structural dimensions [22]. Instead, the fibers used in ECC are tailored [23] to work with a mortar matrix in order to suppress localized brittle fracture in favor of distributed microcrack damage, even when the composite is tensioned to several percent strain. ECC with crack width as low as 30 μm have been made. The ability of ECC to maintain extremely tight crack width in the field has been confirmed in a bridge deck patch repair [24] and in an earth retaining wall overlay [25].

Given the well controlled crack width, Li and coworkers [20,26,27] have investigated the self-healing behavior of ECC under a number of exposure conditions. In their experiments, deliberately pre-cracked ECC specimens were exposed to various commonly encountered environments, including water permeation and submersion, wetting and drying cycles, and chloride ponding. The mechanical and transport properties can be largely recovered, especially for ECC specimens preloaded to below 1% tensile strain. Besides the small crack width, the low water/binder ratio in addition to the large amount of fly ash in their mixture also helps promote self-healing via continued hydration and pozzolanic activities.

In an effort to develop fiber reinforced strain hardening cementitious composites with local waste material and/or byproducts, Zhou et al. [28] at Delft University of Technology have developed a number of mixtures with BFS and LP, all characterized with 2–3% tensile strain capacity and tight crack width (typically below 60 μm). These mixtures are different from that used by Li and coworkers [20,26,27] in the components (e.g. large amount of BFS and LP instead of fly ash) as well as much higher water/binder ratio (0.45–0.60 versus 0.23), which suggests that the amount of unhydrated cementitious material after 28 day curing may be much smaller compared with the samples in their investigations. With similar tight crack width yet very different material components and water/binder ratio, it is therefore interesting to investigate if self-healing still exist in these newly developed materials and if exist, to what extent they can reveal.

In the following sections, the experiment program of this investigation will first be introduced in details, including material preparation, four-point bending test, and microscopic observation using ESEM and XEDS techniques. Furthermore, experimental results on mechanical testing and ESEM observation will be presented and discussed. Finally, overall conclusions will be drawn based on the experimental findings.

2. Experimental programs

2.1. Material proportion and specimen preparation

As shown in Table 1, four mixtures were investigated, including M1–M4. Among the mixtures, M1 is very similar with the ECC developed by Li [22], where fly ash (FA) is used instead of blast furnace slag (BFS) as in M2–M4. Portland cement CEM I 42.5 N was used in the mixture along with BFS and limestone powder. The water to binder (cement + BFS/FA) ratio increases to compensate for the increase of limestone powder content from mixture M1 to M4. The water to powder ratio and superplasticizer content remains nearly constant to reach similar workability for each mixture. The polyvinyl alcohol (PVA) fiber with a length of 8 mm and a diameter of 40 μm was used in the content of 2% by total volume. Fig. 1 shows the particle size distribution of CEM I 42.4 N, BFS and limestone powder.

The solid materials, CEM I 42.5, BFS and limestone powder were first mixed with a HOBART mixer for 2 min thoroughly. Water and superplasticizer were then added and the mixture was mixed at low speed for 1 min, followed by high speed for 2 min. Finally, fibers were added at low speed and the mixture was mixed at high speed for another 2 min. The fresh SHCC was cast into a beam with the dimension of 160 mm × 40 mm × 40 mm for compressive test. Coupon specimens with the dimension of 240 mm × 60 mm × 10 mm were cast for four-point bending and uniaxial tensile tests. After 1 day curing in moulds covered with plastic paper, the spec-

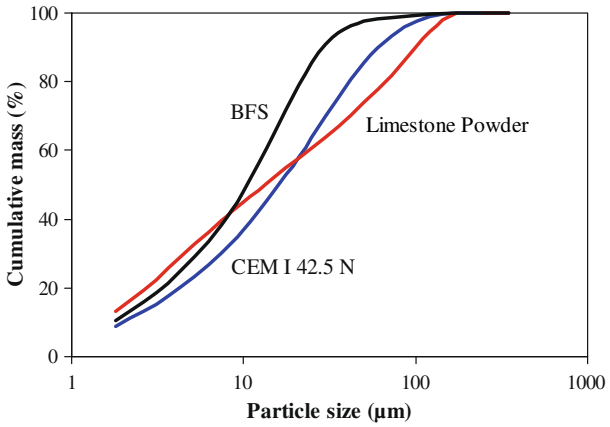

Fig. 1. Particle size distribution of CEM I 42.5 N, BFS and limestone powder.

Table 1
Mix proportion of SHCC.

Mix #	CEM I 42.5 N	Fly ash	BFS	Limestone powder	Water/binder[a] ratio	Water/powder[b] ratio	Super-plasticizer
M1	1	1.2	0	0.8	0.31	0.230	0.033
M2	1	0	1.2	1.5	0.45	0.265	0.023
M3	1	0	1.2	2	0.50	0.260	0.018
M4	1	0	1.2	3	0.60	0.256	0.018

[a] *Binder*: includes both cement and BFS (or fly ash).
[b] *Powder*: includes cement, BFS (or fly ash), and limestone powder.

imens were cured under sealed condition and a temperature of 20 °C for another 27 days before testing.

After 28 days curing, the beam specimen was cut into three cubes with the dimension of 40 mm × 40 mm × 40 mm used in compressive tests. The compressive strength was obtained by averaging the results of three measurements. The coupon specimens were evenly cut into four pieces with the dimension of 120 mm × 30 mm × 10 mm. These specimens were used in a four-point bending test (Fig. 2a). The support span of four-point bending test-setup was 110 mm and the middle span was 30 mm. The flexural strength and deflection were calculated based on the average results of three measurements. The uniaxial tensile tests were carried out on the coupon specimens with both ends directly glued to the Instron machine (Fig. 2b). The testing gauge length was 70 mm and the deformation of specimens was measured with two LVDTs. The tensile load was applied on the ends of coupon specimens at the speed of 0.001 mm/s. Four specimens were tested for each mixture.

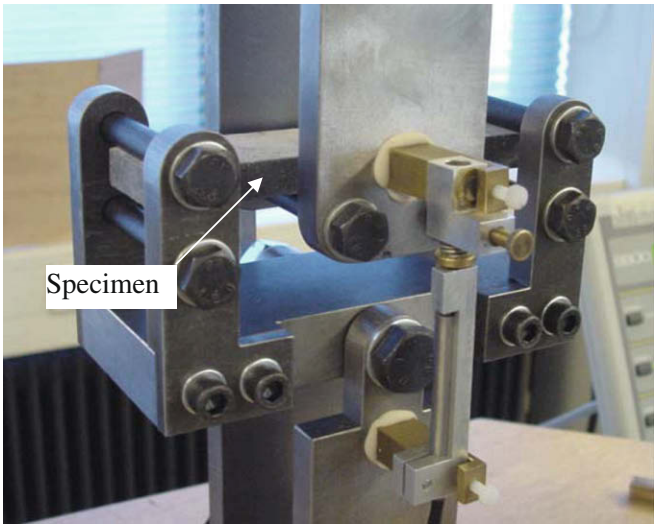

(a)

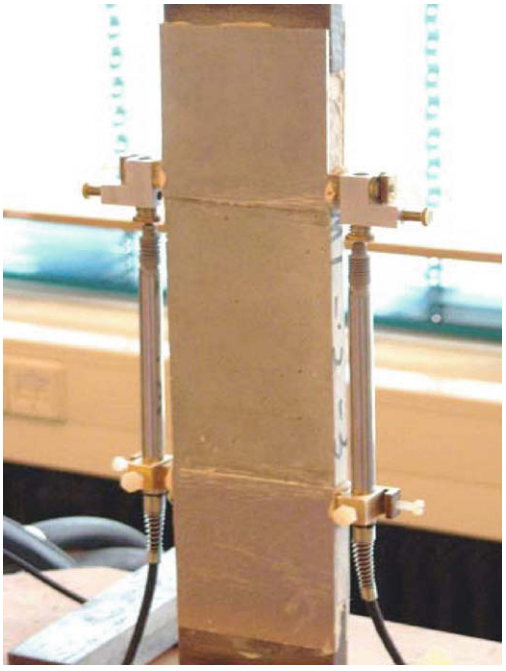

(b)

Fig. 2. Test setup under (a) four-point bending and (b) uniaxial tensile loading.

2.2. Four-point bending

While ideally it is most desirable to use uniaxial tensile test to assess the self-healing behavior in SHCC as the tensile strain hardening behavior represents one of the most important features of SHCC material, the uniaxial tensile test-setup was still under development at the time of this research at Delft University of Technology. The sample from directly gluing method has to be broken and therefore cannot be reused after pre-damage and self-healing process. Therefore it was decided to use four-point bending test (FPBT) to characterize the deflection capacity of SHCC as deflection capacity can also be correlated back to tensile strain capacity so long as the material is truly strain hardening materials [29,30].

The overall program for FPBT is shown in Fig. 3, including three different curing and/or loading schemes. In the first step, all bending samples were first cured under sealed condition (RH 98%) at 20 °C for 28 days after demolding. In the scheme A, three samples of each mixture were tested until final failure to derive the bending strength along with associated ultimate deflection capacity at 28 days. The results from this scheme form a reference value (upper bound) for determining how much healing, especially in terms of deflection capacity, has occurred.

The schemes B and C differ from A since they were not tested to final failure until 56 days. In case of schemes B and C, three samples from each mixture were bent up to 2.4 mm and unloaded at 28 days. The deflection of 2.4 mm (corresponding to tensile strain capacity of approximately 1.7%) is well below ultimate deflection capacity (corresponding to flexural strength) of all three mixtures with no fracture occurred. Afterwards the pre-cracked samples were further cured in water or air (RH 30% at 20 °C), respectively, for 28 more days before testing to final failure. These two schemes are to compare the effect of water and air curing on the self-healing behavior of pre-damaged samples. In the FPBT, the sample was tested under deformation control at a constant rate of 0.01 mm/s.

2.3. ESEM observation and XEDS

The quality of healing is likely influenced by the type of self-healing products formed inside the crack. Analyses of these products were conducted using environmental scanning electron microscopy (ESEM) and X-ray energy dispersive spectroscopy (XEDS) techniques. The crystalline and chemical properties of self-healing products were determined. These techniques are particularly useful in verifying the chemical make-up of self-healing compounds, essential in identifying the chemical precursors to self-healing and ensuring their presence within the composite in future design of the composites.

The failed specimens from bending test schemes B and C were used to prepare samples for ESEM observation. For each mixture,

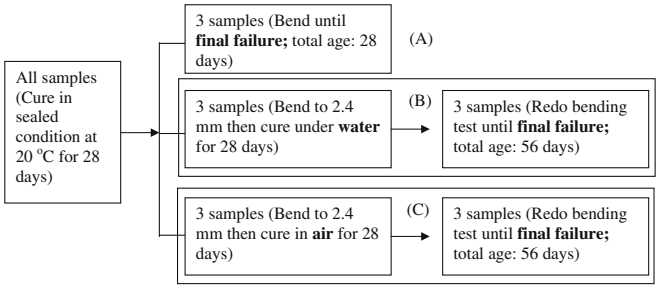

Fig. 3. Bending test program of self-healing cementitious composites.

two samples were prepared for both scheme B and C with at least five microcracks exists in each sample. Firstly, vacuum was employed to dry the sample before epoxy-impregnation. For SEM measurements, the vacuum-dried specimens were impregnated with a low-viscosity epoxy to prevent any loose particles from falling into the crack during surface preparation. After the hardening of epoxy, the specimens were cut with propanediol as cooling agent instead of water. Furthermore, the specimens were carefully ground on the middle-speed lap wheel with p120, p220, p320, p500, p1200 and p4000 sand papers, and were finally polished on the lap wheel with 6, 3, 1 and 0.25 μm diamond pastes. The final polishing was done with a low-relief polishing cloth. Each grinding and polishing step took 2 min. The images were taken with a backscattered electron (BSE) detector with vapor mode. The acceleration voltage of 20 kV was used in order to get a high contrast image.

3. Experimental results and discussion

3.1. Basic mechanical behavior

The compressive and flexural strengths are shown in Fig. 4. As the amount of limestone powder increases and cement decreases, the compressive strength decreases as well from M1 to M4. The flexural strength does not follow this trend exactly, which may be explained that flexural strength is governed by more complex material properties, such as tensile first cracking strength, ultimate tensile strength and tensile strain capacity, particularly in the case of strain hardening cementitious materials.

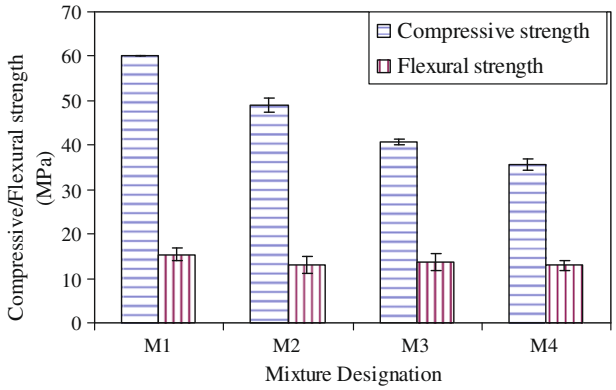

Fig. 4. Compressive and flexural strength of different SHCC materials (compressive strength for M1 is estimated from similar ECC mix from Li [22]).

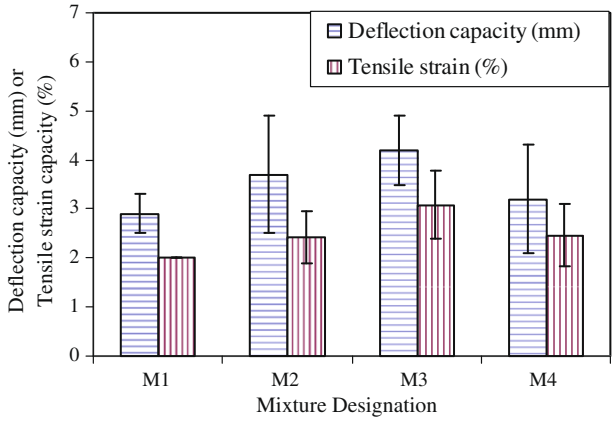

Fig. 5. Comparison of deflection capacity and tensile strain capacity for M1–M4 (only one data point is available for tensile strain capacity for M1).

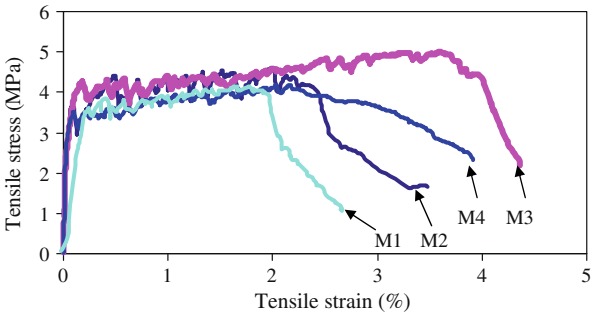

Fig. 6. Typical tensile stress–strain curves of SHCCs.

As shown in Fig. 5, the comparison between the deflection capacity and tensile strain capacity suggests that there is a relatively good correlation between these two properties. This is expected as Qian and Li [29] found that the deflection capacity can be linearly correlated with tensile strain capacity. Therefore deflection capacity can be used in practice for quality control of SHCC type material due to the simplicity of four point bending test as long as the material has been pre-qualified as truly strain hardening material. The typical tensile stress–strain curves for different SHCCs are shown in Fig. 6, where all mixtures showing a tensile strain capacity of at least 2–4%, which is about 200–400 times that of normal concrete. Typical crack pattern from the tensile face of the bending sample and tensile sample is shown in Fig. 7. Notice the width of sample (parallel to the crack orientation) is 30 mm and 60 mm, respectively.

3.2. Recovery of mechanical properties

3.2.1. Deflection capacity

The deflection capacity is of major concern for SHCC type material since its structural application mainly requires high deformation and energy dissipation capacity. The deflection capacity herein is defined as the deflection that corresponds to maximal flexural stress, i.e. flexural strength in flexural stress–deflection curve. In the experiment program, three schemes have been carried out to investigate the influence of water and air curing on the recovery of deflection capacity.

As can be seen in Fig. 8a, deflection capacity from different mixtures under different test scheme clearly reveals the recovery of deflection capacity from all mixtures, especially for M1, M2 and M3. Compared with scheme C, scheme B shows significant improvement of deflection capacity; in some case it even exceeds the performance of reference (M1). This recovery of deflection capacity suggests that the water curing have greatly promoted the self-healing process and therefore enhanced the fiber bridging behavior after pre-cracking while it is not the case for air cured pre-cracked samples.

Similar trend can be seen from the normalized deflection capacity as shown in Fig. 8b, where all deflection capacity was normalized by that of scheme A. The deflection capacity from self-healed specimens (scheme B) reaches about 65–105% that of the virgin specimen (scheme A) despite of a preloaded deflection of 2.4 mm. Conversely, the air cured specimens (scheme C) show about 40–62% of deflection capacity of the virgin specimen.

Based on the limited data in this study (Fig. 9), it appears that the normalized deflection capacity of scheme B decreases as the water/binder ratio and powder/binder ratio increases from M1 to M4 (Table 1). Since normalized deflection capacity can be seen as the self-healing performance indicator of different mixture with respect to the reference scheme A, Fig. 9 therefore also suggests that under scheme B the self-healing capacity decreases as the

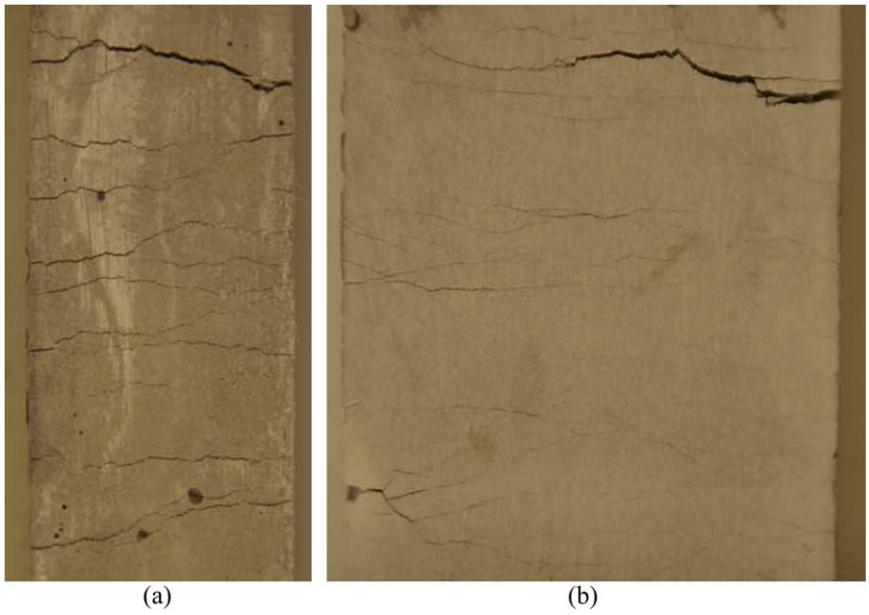

Fig. 7. Specimen crack pattern of (a) bending sample (30 mm wide) and (b) tensile sample (60 mm wide).

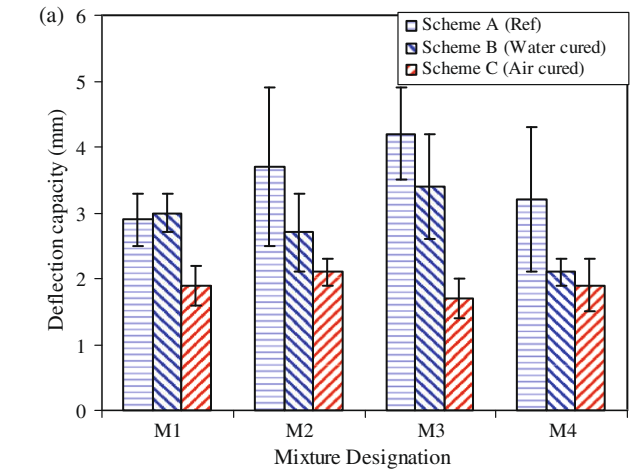

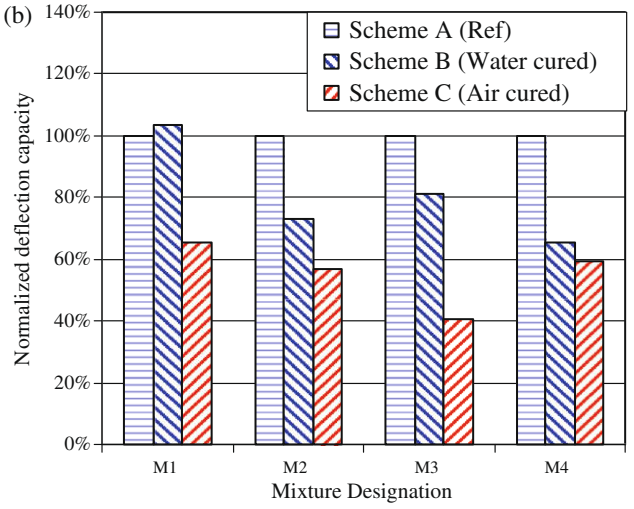

Fig. 8. Comparison of (a) deflection capacity and (b) normalized deflection capacity from different mixtures (normalized by the deflection capacity with scheme A).

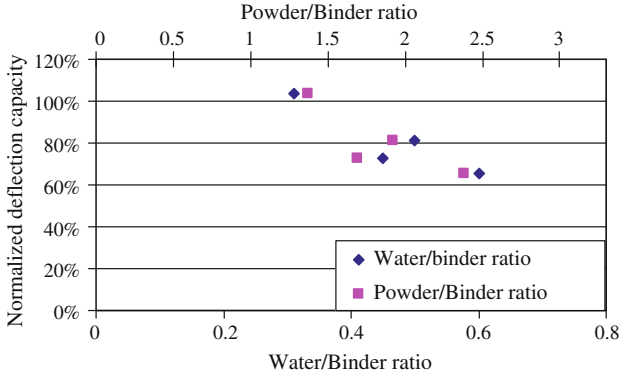

Fig. 9. Influence of powder/binder and water/binder ratio on the normalized deflection capacity after healing (scheme B).

water/binder ratio and powder/binder ratio increases from M1 to M4. This can be explained that as the water/binder ratio and powder/binder ratio increases from M1 to M4, the reservoirs of unhydrated cement and unreacted cementitious material will decrease, therefore making it more difficult for self-healing to take place.

3.2.2. Deflection hardening behavior

The recovery of deflection hardening behavior for scheme B can be clearly observed from Fig. 10, where the bending stress–deflection curves were presented for all mixtures under different schemes, including bending stress–deflection curves from pre-cracking. As expected, sample from scheme A (virgin reference sample) shows a typical deflection hardening behavior for all mixtures M1–M4. The deflection curve for scheme A is characterized by an initial linear curve up to the cracking strength of various mixtures, followed by a bend over and subsequent plateau curve with a relatively small hardening modulus until final fracture. The large nonlinear portion of the deflection curve corresponds to the continuous microcracking process of the specimens.

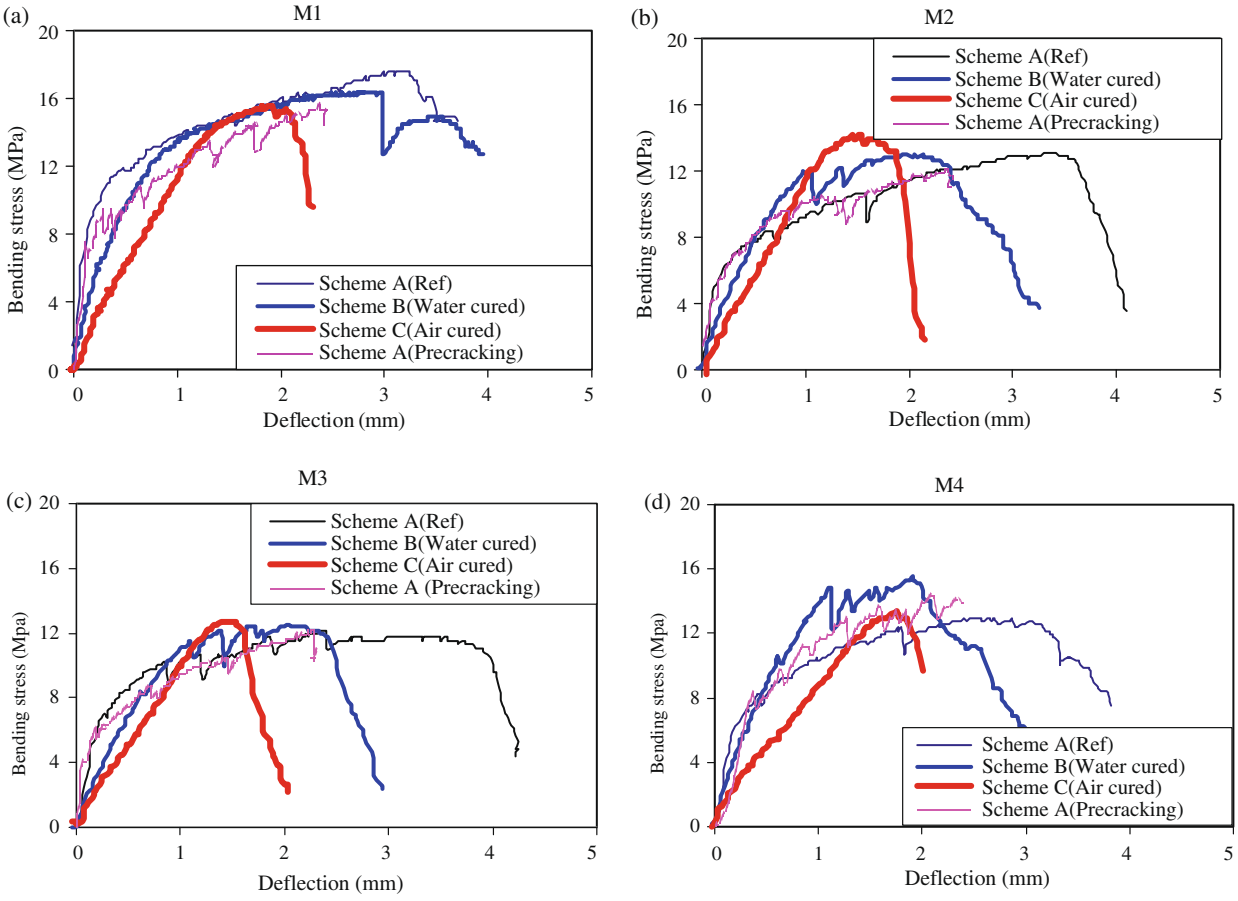

Fig. 10. Comparison of typical bending behavior under different curing schemes for (a) Mix 1, (b) Mix 2, (c) Mix 3 and (d) Mix 4.

Similarly, the curves corresponding to scheme B reveal characteristics of deflection hardening behavior, namely a more or less linear curve followed by a plateau curve. Unlike the linear curve in scheme A, where the virgin sample is in fully elastic loading stage, the linear curve in the scheme B is largely due to the reopening of the microcracks from previously loading. The following plateau curve results from the continuous cracking process from new defect sites and relatively strong self-healed crack.

On the contrast, the curves from scheme C shows very little sign of deflection hardening. Once the linear stage ends, the deflection curve bend over and final fracture takes place shortly thereafter. This suggests that there are not many new cracks developed besides the reopening of old microcracks from pre-loading. From the comparison of the bending stress–deflection curves of scheme B and C, it again suggests that water curing does enhance the fiber bridging inside the preexisting microcracks, which in turn facilitate the extended cracking from self-healed microcrack and new defect sites.

3.2.3. Stiffness and flexural strength

Additionally, the effect of self-healing can also be seen from the enhanced stiffness of the water cured sample compared with air cured sample. As revealed in Fig. 10, the stiffness of the initial linear stage of scheme B is always larger compared with that of scheme C. This can be plausibly explained by the strengthening effect of self-healing products which make the preexisting crack more difficult to open in the scheme B, while there is no such strengthening effect exists in the scheme C. This will be further confirmed by the observations of the ESEM study presented in the next section.

Furthermore, the stiffness of the initial linear stage of scheme B is always smaller than that of virgin specimen in scheme A (Fig. 10). This is as expected, as from the literature, the main component of self-healing products are usually calcium hydrates or calcium carbonates, which is typically weaker than that of CSH from the cement hydration. Even if CSH is formed inside the crack due to rehydration of unhydrated cement, the bond strength between the crack surface and new CSH is most likely to be weaker compared with the cracking strength of virgin sample.

The flexural strength from different mixture under different schemes is compared in Fig. 11. The flexural strength from scheme

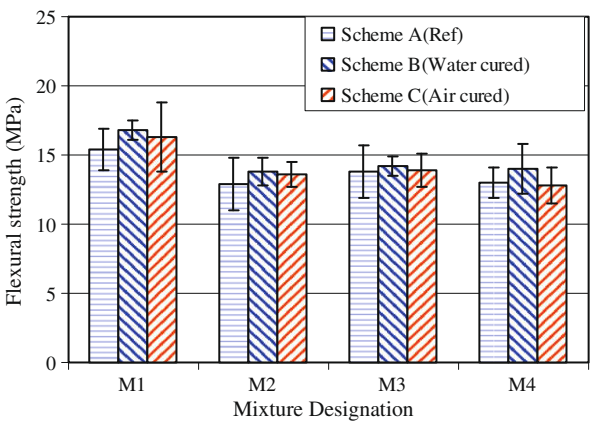

Fig. 11. Comparison of flexural strength from different mixture.

B and C generally shows negligible difference when compared with that of scheme A. The flexural strength was not reached during pre-cracking in schemes B and C, hence the final fracture plane which dominates the flexural strength has not opened during pre-cracking process. Therefore the flexural strength should remain constant regardless of the process of pre-cracking, which is revealed in the figure.

3.3. ESEM observation and XEDS

Typical crack pattern after healing can be seen in Fig. 12a, where the preexisting crack can barely be seen. These cracks are covered by some white residue presumably due to the healing process under water curing. On the contrast, there is no such white residue exists on the sample that is air cured. While most of the crack under reloading passes through the preexisting crack, some crack does deviate from the preexisting crack and sometimes even new crack forms while the surrounding old crack shows little or no opening (Fig. 12b). This event, while relatively rare, demonstrated the ultimate possibility of mechanical self-healing in the SHCC type material and has also been observed by Li and Yang [20].

While it is interesting to have an overview of the crack pattern of healed specimen after water curing, more detailed information such as chemical make-up of healing products, extent of healing, etc can only be obtained by more advanced techniques, e.g. environmental scanning electron microscopy (ESEM) and X-ray energy dispersive spectroscopy (XEDS) techniques. The investigations using above techniques will be presented in the following sections.

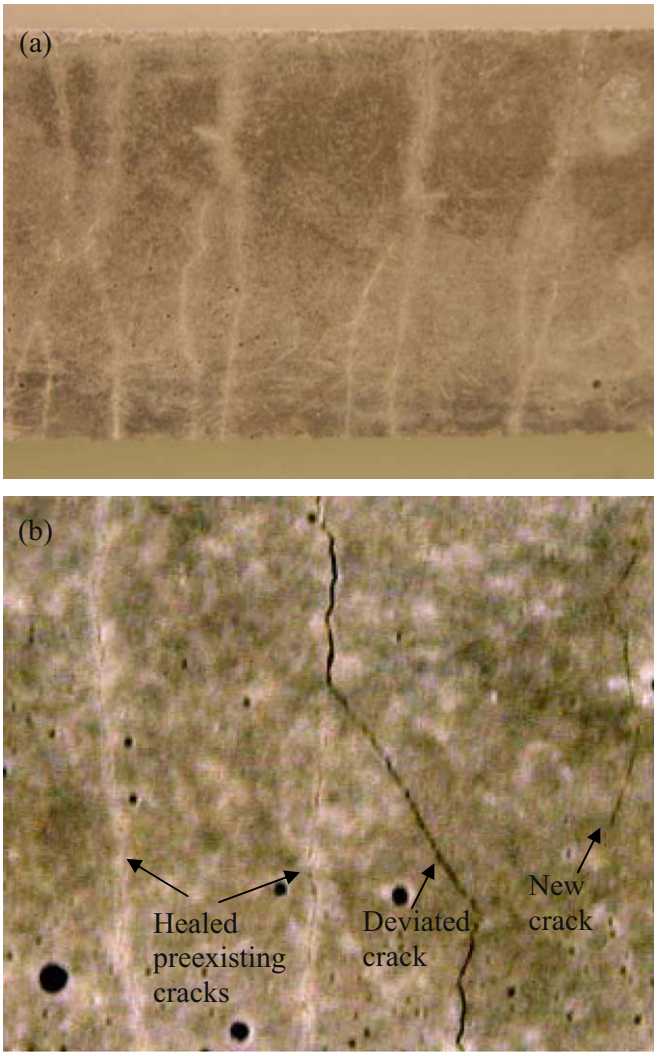

Fig. 12. Self-healed specimen (a) before and (b) after retest.

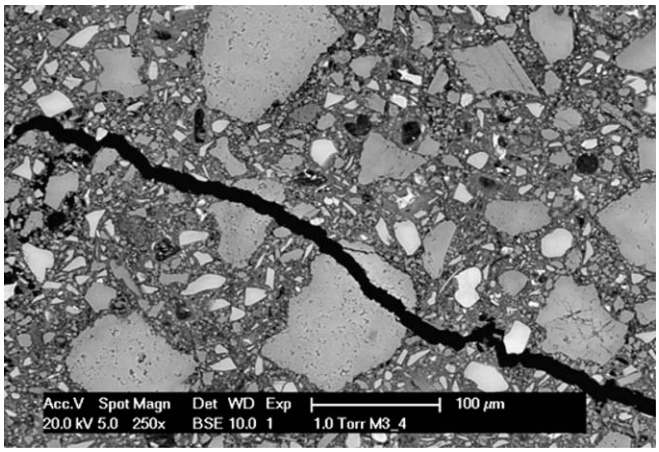

Fig. 13. Air-cured sample.

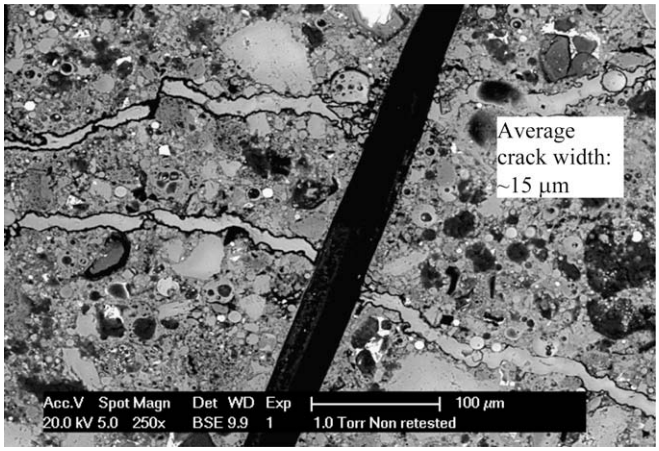

Fig. 14. Precracked sample after water curing (no reloading applied).

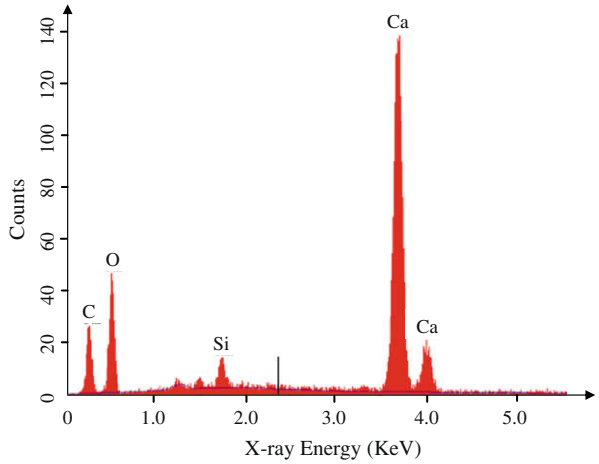

Fig. 15. ESEM surface chemical composition analysis (XEDS) of healing products inside the microcracks.

ESEM pictures (with BSE detector) for typical air cured and water cured samples are compared in Figs. 13 and 14. The air cured sample reveals no sign of healing, while water cured sample appears to be completely healed, where two microcracks are fully filled with healing products (Fig. 14). Surface chemical composition analysis via XEDS reveals that the main composition of the healing products inside the microcrack is calcium carbonate (Fig. 15). To facilitate healing of the cracks, and promote formation of calcium carbonate, the calcium hydroxide from cement hydration has to be leaching out of the bulk material into cracks and react with carbon dioxide. Without the presence of water, this leaching process will not be possible, which is evident from the ESEM observation of the air cured samples.

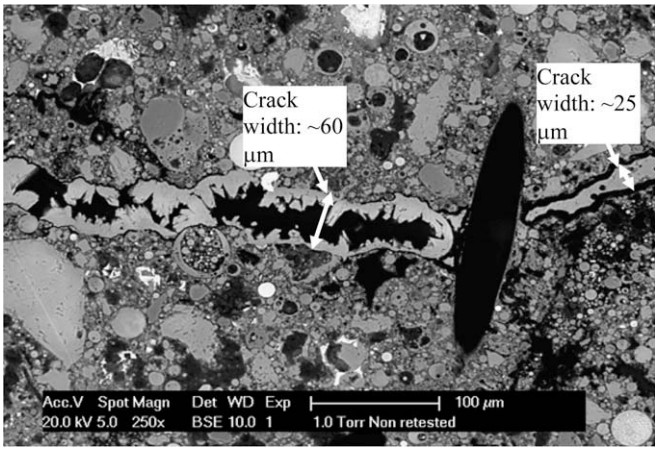

Fig. 16. Partial crack healing after water curing.

Moreover, partially healed crack in Fig. 16 suggests that the healing products grow from both surfaces of the crack towards the middle of the crack. This may be explained by the relatively high concentration of calcium hydroxide near the crack surface and the fractal surface which may serve as the calcite nucleation sites. While most of the cracks (crack width ranges from 10 to 60 μm) fully healed, a few crack with relatively large width (60 μm) did show partial healing, as evident in Fig. 16. For smaller crack width, such as those in Figs. 14 and 16, the cracks are always completely healed. This tendency suggest that crack with smaller width are preferable as far as the self-healing is concerned, as it requires much less healing products to fill the crack and much easier for the healing products to grow from both faces of the crack to get connected.

The effect of self-healing in enhancing fiber bridging and therefore deflection capacity after pre-cracking can be vividly revealed in Fig. 17. In the figure, two preexisting cracks were both healed and one crack reopened after reloading. Without the self-healing in the microcracks, the fiber would have no bridging effect for the opening of the microcrack since the fiber embedment length appears to end near the rehealed crack. While this is an extreme case among all the fibers bridging crosses the crack, the effect of healing on restoration of the fiber bridging on the micro-scale and consequently the composite ductility on the macro-scale is evident. This further confirmed previous experimental findings on the improvement of deflection capacity after water curing. To quantitatively link the restoration of fiber bridging after self-healing with enhancement of composite behavior at the macro-scale, more detailed experiments on micro- or meso-scale, such as single fiber pullout test, fiber bridging across single crack test before and after healing is needed.

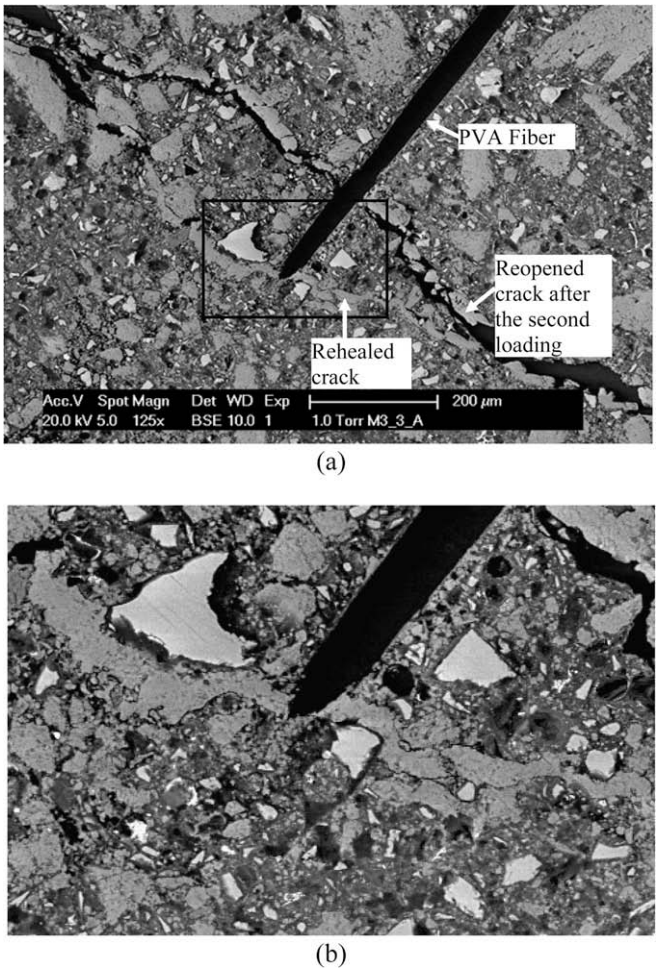

Fig. 17. (a) Enhanced crack bridging due to self-healing and (b) close-up view of the framed part in (a).

4. Conclusions

Self-healing behavior of pre-cracked SHCC with local waste materials (BFS and LP) is investigated in this paper. Four-point bending tests are used to precrack SHCC beam specimens deflected up to 2.4 mm with subsequent curing in water and air for 28 days. The sample submerged in water shows greatly enhanced deflection capacity as well as stiffness recovery due to the healing products presented in the microcrack, while this is not the case for specimens cured in air. The ESEM and XEDS observation further confirmed the finding in mechanical tests. The self-healing cementitious composites developed in this research can potentially reduce or even eliminate the maintenance needs of civil infrastructure, especially when repeatable high deformation capacity is desirable, e.g. bridge deck link slabs and jointless pavements. The following conclusions can be drawn based on this investigation:

1. For specimens submerged in water, the deflection capacity after self-healing can recover about 65–105% compared with those virgin specimens, while this ratio is about 40–60% for air cured specimens. Furthermore, the stiffness of initial linear stage of self-healed specimen is much larger compared with that of the air cured specimen due to the presence of healing products formed inside the crack and strengthened the bridging fiber.
2. The observations under ESEM and XEDS confirm that the microcracks submerged in water were healed mainly with calcium carbonate. ESEM also suggests that the healing products grow from both faces of the crack towards the middle of the crack.

This may be explained by the relatively high concentration of calcium hydroxide near the crack surface via diffusion process from the bulk cementitious material.

3. While SHCC materials used in previous studies of self-healing were characterized with high percentage of fly ash and low water/binder ratio, SHCC in this study was made with large amount of BFS, LP along with relatively high water/binder ratio. Nevertheless, the new SHCC materials developed with local waste materials (BFS and LP) still preserve similar self-healing behavior due to tight crack width.
4. Self-healing behavior in SHCC heavily depends on the availability of unhydrated cement and other supplementary cementitious materials, such as BFS. Low water/cementitious material ratio and high percentage of cementitious material appear to promote self-healing behavior.
5. Microcrack with smaller crack width as in the SHCC mixtures is preferable as far as continuous hydration-based self-healing is concerned, as it requires much less healing products to fill the crack and much easier for the healing products to grow from both faces of the crack to get connected.

Acknowledgements

The authors would like to thank Dutch Ministry of Economic Affairs for their financial support for this work (IOP Self-healing Materials – Healing Built-in Building Materials).

References

[1] Nijland TG, Larbi JA, van Hees RPJ, Lubelli B, de Rooij MR. Self-healing phenomena in concretes and masonry mortars: a microscopic study. In: van der Zwaag S, editor. Proceedings (CD) first international conference on self-healing materials. Dordrecht: Springer; 2007.
[2] Edvardsen C. Water permeability and autogenous healing of cracks in concrete. ACI Mater J 1999;96(4):448–55.
[3] Reinhardt H, Joos M. Permeability and self-healing of cracked concrete as a function of temperature and crack width. J Cem Concr Res 2003;33:981–5.
[4] Ter Heide N, Schlangen E, van Breugel K. Experimental study of crack healing of early age cracks. In: Proceedings Knud Hojgaard conference on advanced cement-based materials: research and teaching. Lyngby, Denmark; 2006.
[5] Pimienta P, Chanvillard G. Retention of the mechanical performances of Ductal specimens kept in various aggressive environments. In: Fib symposium; 2004.
[6] Granger S, Pijaudier-Cabot G, Loukili A. Mechanical behavior of self-healed ultra high performance concrete: from experimental evidence to modeling. In: Proceedings FRAMCOS 6, Catalina. Italy; 2007.
[7] Sahmaran M, Keskin SB, Ozerkan G, Yaman IO. Self-healing of mechanically-loaded self consolidating concretes with high volumes of fly ash. J Cem Concr Compos 2008;30(10):872–9.
[8] White SR, Sottos NR, Geubelle PH, Moore JS, Kessler MR, Sriram SR, et al. Autonomic healing of polymer composites. Nature 2001;409:794–7.
[9] Kessler MK, Sottos NR, White SR. Self-healing structural composite material. Compos Part A: Appl Sci Manuf 2003;34(8):743–53.
[10] Dry C. Matrix crack repair and filling using active and passive model for smart time release of chemicals from fibers into cement matrixes. J Smart Mater Struct 1994:118–23.
[11] Li VC, Lim YM, Chan Y. Feasibility study of a passive smart self-healing cementitious composite. Composites Part B 1998;29(B):819–27.
[12] de Rooij MR, Qian S, Liu H, Gard WF, van de Kuilen JWG. Using natural wood to heal concrete. In: 2nd International conference on concrete repair, rehabilitation and retrofitting, Cape Town, South Africa; 2008.
[13] Kishi T, Ahn TH, Hosoda A, Suzuki S, Takaoka H. Self-healing behavior by cementitious recrystallization of cracked concrete incorporating expansive agent. In: van der Zwaag S, editor. Proceedings (CD) first international conference on self-healing materials. Dordrecht: Springer; 2007.
[14] Bang SS, Galinat JK, Ramakrishnan V. Calcite precipitation induced by polyurethane-immobilized *Bacillus pasteurii*. Enzyme Microb Technol 2001;28:404–9.
[15] Jonkers HM, Schlangen E. Crack repair by concrete-immobilized bacteria. In: van der Zwaag S, editor. Self-healing materials. Dordrecht: Springer; 2007. p. 95–204.
[16] Clear CA. The effects of autogenous healing upon the leakage of water through cracks in concrete. In: Cement and concrete association technical report no. 559; 1985.
[17] Jacobsen S, Marchand J, Homain H. SEM observations of the microstructure of frost deteriorated and self-healed concrete. J Cem Concr Res 1995;25:1781–90.
[18] Ismail M, Toumi A, Francois R, Gagne R. Effect of crack opening on local diffusion of chloride inert materials. J Cem Concr Res 2004;34:711–6.
[19] Aldea C, Song W, Popovics JS, Shah SP. Extent of healing of cracked normal strength concrete. J Mater Civil Eng 2000;12:92–6.
[20] Li VC, Yang E. Self-healing in concrete materials. In: van der Zwaag S, editor. Self-healing materials. Dordrecht: Springer; 2007. p. 161–93.
[21] ACI Committee 318. Building code requirements for structural concrete and commentary. American Concrete Institute 318; 2008. 430p.
[22] Li VC. On engineered cementitious composites (ECC) – a review of the material and its applications. J Adv Concr Technol 2003;1(3):215–30.
[23] Li VC, Wu C, Wang S, Ogawa A, Saito T. Interface tailoring for strain hardening PVA–ECC. ACI Mater J 2002;99(5):463–72.
[24] Lepech MD, Li VC. Long term durability performance of engineered cementitious composites. Int J Restor Build Monum 2006;12(2):119–32.
[25] Kunieda M, Rokugo K. Recent progress on HPFRCC in Japan, required performance and applications. J Adv Concr Technol 2006;4(1):19–33.
[26] Yang Y, Lepech M, Li VC. Self-healing of ECC under cyclic wetting and drying. In: Proceedings of International workshop on durability of reinforced concrete under combined mechanical and climatic loads, Qingdao, China; 2005. p. 231–42.
[27] Sahmaran M, Li M, Li VC. Transport properties of engineered cementitious composites under chloride exposure. ACI Mater J 2007;104(6):604–11.
[28] Zhou J, Qian S, Sierra Beltran MG, Ye G, Schlangen E, van Breugel K. Developing Engineered Cementitious Composite with local materials. In: International conference on microstructure related durability of cementitious composites, Nanjing, China; 2008.
[29] Qian S, Li VC. Simplified inverse method for determining the tensile strain capacity of strain hardening cementitious composites. J Adv Concr Technol 2007;5(2):235–46.
[30] Qian S, Li VC. Simplified inverse method for determining the tensile properties of strain hardening cementitious composites. J Adv Concr Technol 2008;6(2):353–63.